SLAC-PUB--6064

DE93 010953

LCLS OPTICS: SELECTED TECHNOLOGICAL ISSUES AND SCIENTIFIC OPPORTUNITIES *

ROMAN TATCHYN

Stanford Linear Accelerator Center
Stanford Synchrotron Radiation Laboratory
Stanford University, Stanford, CA 94309

Abstract

The Stanford Linac Coherent Light Source (LCLS) promises to generate photon pulses of unprecedented brevity and peak brightness in the soft x-ray range. In this presentation selected limitations and novel opportunities for technology and science associated with the availiability of such pulses will be briefly assessed. Special emphasis will be placed on possible techniques for extending the peak power density and the temporal and spectral regimes of the LCLS output radiation by orders of magnitude beyond their nominal (calculated) values, and to the associated instrumentation for processing this radiation.

---

* Work supported in part by the US DOE Offices of Basic Energy Sciences and High Energy and Nuclear Physics and the US Department of Energy under contract DE-AC03-76SF00515

Presented at the Workshop on Scientific Applications of Short-Wavelength Coherent Light Sources, Stanford, CA, October 21, 1992.

LCLS OPTICS: SELECTED TECHNOLOGICAL ISSUES AND SCIENTIFIC OPPORTUNITIES*

Roman Tatchyn

Stanford Synchrotron Radiation Laboratory, Stanford Linear Accelerator Center, Stanford, CA 94305, USA

Abstract

The Stanford Linac Coherent Light Source (LCLS) promises to generate photon pulses of unprecedented brevity and peak brightness in the soft x-ray range. In this presentation selected limitations and novel opportunities for technology and science associated with the availability of such pulses will be briefly assessed. Special emphasis will be placed on possible techniques for extending the peak power density and the temporal and spectral regimes of the LCLS output radiation by orders of magnitude beyond their nominal (calculated) values, and to the associated instrumentation for processing this radiation.

*Supported by DOE Offices of Basic Energy Sciences and High Energy and Nuclear Physics

I. LCLS output characteristics

In recent work, systematic studies of various linac-driven Free-Electron Laser (FEL) configurations, primarily in the vicinity of the water window (≈40 Å), based on excitation with a laser-excited photocathode electron gun, were conducted [1]. A comprehensive list of the associated system parameters for selected configurations at this and substantially differing wavelengths may be found in the columns under the "RF Gun Based" heading in Figure 1. Brief definitions of the descriptive parameters are shown in Fig. 2. From the rows labelled "σ_s," "$E_{\lambda\,(coh)}$," "DIAM. @ 50m," and "DIAM. @ 250m," the peak output power density at normal incidence can be estimated to lie in a range of 10^{11}-10^{12} W/cm^2, at associated (full) pulse lengths of ≈ 0.5 ps. In addition to the major coherence parameters listed in Fig. 1, these may be taken as the nominal output parameters of the (water-window) LCLS running at 6 GeV.

An important property of the electron bunch accelerated through the linac is the development of an energy gradient (or "correlated energy spread") in the forward direction due to electrons in the front of the bunch loading the accelerating fields addressed by the trailing particles [2]. This energy spread is superimposed on the "uncorrelated" energy spread of the bunch characterized by its (stochastic) emittance parameters. For our purposes, we note that these energy spreads show up as, respectively, "inhomogeneous" and "homogeneous" line broadenings in the FEL photon pulse. Due to the γ^2 (or E^2) dependence of the

FEL's output photon energy, these broadenings can be shown to appear with roughly twice the relative size in the photon spectrum as in the electron bunch.

In the following parts of our presentation we will address: 1) selected peak intensity and materials damage issues; 2) peak intensity damage mitigation using a) solid-state materials in grazing incidence configurations, b) gas optics, or c) disposable optics; 3) pulse-length limitations on monochromator performance; 4) enhanced monochromatization via pulse lengthening; 5) LCLS pulse compression techniques based on the linac-induced correlated energy spread and selected applications; and 6) power density enhancement via microfocussing and selected applications.

2. Peak intensity and materials damage

At normal incidence, it is easy to estimate from typical attenuation coefficients in the soft x-ray range [3] and the tabulation in Figure 1 that 1 eV or more of energy can be deposited per atom in 0.5 ps. Apart from photoemission, which typically accounts for only a few-to-several percent of the absorbed energy, the primary energy-removal channels (radiation, conduction, etc.) all have time constants that are considerably longer. Keeping in mind that typical atomic or molecular lattice binding energies are of the order of 1 eV, we can appeal to the "pigeonhole principle" to infer that the probability of atomic an

molecular bonds beginning to break and the absorbed energy being transported away by fragmentation must start becoming appreciable under the cited conditions. We can consequently expect enhanced probability of damage in solid state materials by the LCLS photons from two primary effects: 1) lattice disruption/ablation, and 2) photoemissively-generated field stresses.

It should be noted that the enhanced probability of structural damage and ablation is likely to be particularly important with regard to the LCLS beam line optics, or, more generally, for samples in which the same area gets repeatedly irradiated, effectively integrating the probability of damage over long periods of time. For example, even if the probability of any irradiated atom ablating is as low as 1 part in 10^7 per pulse, substantial damage to an optical surface could be expected after only 10 hours of operation at a 120 Hz rep rate. We may note here that both lattice disruption and ablation can in principle be highly deleterious to the performance of multilayer optics, especially those with small periods. Photoemissively-induced field stresses, which clearly merit a more systematic and detailed study, will also affect the design and operating strategy of optical elements and experimental samples. For example, to enhance the rate of charge neutralization, one would probably want to avoid using mirrors (even at grazing incidence) consisting of thin metallic films deposited on dielectric or semiconducting substrates with large areas.

3. Special techniques for peak intensity damage mitigation

The most intuitively evident way to mitigate peak intensity damage is to dilute the energy deposited per unit area (and thereby per atom) by the artifice of grazing incidence. General parameters associated with this approach for specular reflectors are shown in Figs. 3-5. We note the quantitative definition of η [eV/atom] in terms of the LCLS parameters, the grazing-incidence parameters, and the physical constants (including the reflectivity R) of the mirror material. Since the grazing-incidence geometry is necessary to attain high values of R in the soft x-ray range, we also see that good optical performance and intensity-related damage inhibition are mutually consistent in this energy range. This result may be only partially generalized to multilayer reflectors, where smaller grazing incidence angles imply thicker periods, resulting not only in lesser damage, but in lesser sensitivity of performance to damage. Unfortunately, the typically large absorption of many multilayer materials in the soft x-ray range will also tend to restrict the reduction of the grazing incidence angle to overly small values, where the diminishing reflectivity may start countering the effects of the grazing-incidence dilution of η.

The methods outlined in Figs. 3-5 have currently been applied to generate a practical design for a mirror station for the LCLS, which has been described during the course of the workshop.

Notwithstanding the apparent effectiveness of grazing-incidence optics for the given LCLS parameters and the

assumed spectral range, future x-ray FEL configurations can be posited (e.g., the tapered wiggler [4]) whose peak outputs might be too high to be adequately handled by solid-state specular reflection even at extreme grazing incidence. To this end, we can consider two additional options: 1) gas optics, and 2) disposable normal-incidence optics.

Two possible schemes utilizing gas optics are shown in Fig. 6. The first, a "gas prism" deflects the LCLS output beam by inducing a phase gradient in its wavefront, similarly to an ordinary optical prism. The major difference lies in the rather large differential attenuation accompanying the phase gradient, which is seen to incur an appreciable intensity-loss penalty per degree of deflection. Numerical studies indicate that this penalty is virtually prohibitive for all gases but hydrogen and helium, and is rather severe even for the former. An alternative possibility would be to configure a "gas grating" with period a, enabling a minimum deflection angle of λ/a to be attained. Here, however, the relative efficiency of the diffracted orders will be determined by the density contrast attained in the gas and their absolute efficiency by the average gas thickness, and it will probably prove to be difficult to generate thin gas sheets with significant density or particle-number contrasts for grating periods extending down to 10μ and beyond. We can also note here that although fully or partially ionized plasmas could in principle offer more advantageous optical constants for effective beam steering, the preparation of sufficiently small and dense jets would in general be expected to be significantly more difficult than with unionized

gases.

Given these observations, we note that the relatively sparse pulse structure (120 Hz) of the LCLS can easily allow mechanical motion of optical surfaces and shutters over distances significantly greater than the beam waist to occur between pulses. This makes feasible the notion of using "disposable" optics at normal or near-normal incidence to deflect or otherwise process the LCLS beam. For example, with a beam spot size of 1 mm, we can estimate that if the 1 mm area of impact is totally obliterated by one pulse, we would require a renewal rate of the optical surface of about 1 m^2/hour. For ultra-thin optics (e.g., zone plates or transmission gratings), suitably-placed rotating shutters could be used to effectively trap and collect the debris, and recovery and re-fabrication schemes could perhaps be developed to sustain economic feasibility. With regard to the numerous comments made at this workshop concerning experimental limitations caused by damage to solid state or liquid samples, we note that a similar "inter-pulse" scanning stratagem could be used to significantly ease the apparent restrictions. To wit, rather than probing one sample only (as is conventionally done), one could prepare, say, N identical samples (viz., an experimental ensemble) and "step" them through successive LCLS pulses. This would amount to introducing an additional (statistical) degree of freedom into the LCLS experimental algorithm, and would - especially for large N - tend to be more costly and involved than using just one sample. However, the increase in the dynamic range of otherwise conventional parameter space gained by this approach should allow

the systematic probing of high-intensity physical phenomena inaccessible by other techniques at alternative SR facilities.

4. Pulse-length limitations on attainable coherence

Under the condition that the correlated and uncorrelated energy spreads in the electron bunch are equal, the FEL radiation spectrum will be broadened to more than twice its natural relative width (ρ_{eff}). For larger correlated energy spreads the inhomogeneous broadening will be correspondingly greater. The present lack of detailed knowledge of the actual spread in the width of the LCLS pulses underscores the desirability of being able to monochromatize the emitted FEL photon pulses, and a number of important scientific applications such as, e.g., high-precision absorption or photoemission spectroscopy, will demand it.

As indicated in Figs. 7 and 8, conventional soft x-ray monochromators usually process temporal pulses that are considerably longer than the coherence length of the wave trains corresponding to their resolving power. For the LCLS, however, the pulse length could approach or even become smaller than this coherence length. For example, if the FEL pulse length is 0.1 ps long, this corresponds to 7500 wavelengths of 40 Å light, and the resolution attainable by a conventional monochromator designed to attain a resolution of, say, 10^{-4} at this wavelength could not exceed 1/7500. A geometrical outline of the propagation of this effect is sketched at the bottom of Fig. 7 and a tabulation of

typical pulse length loading on attainable resolving power is given in Fig. 8.

The natural way to try to improve the situation is, evidently, to devise schemes for lengthening the LCLS pulse. As can be seen in the bottom schematic of Fig. 7, the diffraction process itself can be used to lengthen the pulse diffracted into any order, along with a corresponding increase in angular spread. By selecting a small fraction of the dilated pulse with suitable angular filtering, one can obtain an attenuated and dilated pulse suitable for further monochromatization. It is evident that methods like these, based on dispersive and angular filtering, will discard significant fractions of the emitted in-band photons; however, the initially high values of this parameter in the LCLS pulse should make their implementation potentially useful and interesting. An alternative approach, which would also result in significantly fewer in-band photons, would be to underutilize the compression stages in the accelerator to produce longer electron bunch lengths with smaller peak currents.

5. Pulse compression techniques for the LCLS

As stressed elsewhere in this workshop (e.g., Refs. [5-6]), the sub-picosecond temporal structure of the LCLS as contrasted with those of conventional synchrotron radiation (SR) facilities promises to open up important new avenues for scientific research in photon-based spectroscopies and other areas. At the same time,

specialized applications such as, e.g., the study of molecular and chemical dynamics were identified that could benefit from x-ray pulse lengths as short as 10-15 fs [7]. To this end, it is important to point out that different methods of shortening the LCLS pulses to values beyond those listed in Fig. 1 might be applicable. Perhaps the most direct approach would be to compress the electron bunch even further. Preliminary assessments indicate that another factor of 10 (viz., down to 50 fs) could perhaps be feasible [8]. This method, while non-trivial to implement, would evidently be the most attractive, since it would deliver the maximum number of in-band photons to the experimenter. Apart from developments associated with the electron bunch, it is useful to note that the inhomogeneous energy gradient of the photon beam in the forward direction could also be used to extract x-ray pulses from the LCLS with durations down to 100 fs range and beyond. The method for accomplishing this, based on dispersion by a transmission grating with a chirped period at normal incidence, is schematized at the top of Fig. 9. Table 2 in Fig. 9 shows some of the attainable pulse lengths (τ_c'), required inhomogeneous energy spreads, grating line densities, and expected loss factors associated with the proposed technique.

6. Microfocussing and selected applications

A research program aimed at developing and exploiting high-intensity SR and its coherence properties has been in

progress at SSRL since 1983. One initial goal of the program has been the development of optics and physical systems for pumping soft x-ray transitions in atomic Lithium with SR with the ultimate aim of producing a soft x-ray laser at 66 eV [9]. To this end, an ellipsoidal "superfocussing" specular reflector was designed and fabricated and in a series of experiments power densities of 10^9 Watts/cm^2 were attained (see Fig. 10) at Beam Line 5 on SPEAR. In the literature reporting on this work [10], a number of potential experimental applications of SR beams microfocussed down to densities of 10^{10}-10^{12} Watts/cm^2 were noted, including: 1) pumping of soft x-ray transitions in solids, liquids, and gases, 2) study of non-linear phenomena associated with outer and inner-shell processes, 3) "flash" holography and microscopy of living organisms, 4) microprobing, and 5) the study of saturation effects in surface and bulk photoemission. Due to unfavorable emittance parameters on SPEAR, which limited the attained power density, plans were developed for a soft x-ray insertion device facility on PEP [11,12] which was expected to attain the microfocussed power densities required for the cited research. It is noteworthy that we now expect that the power densities that were once anticipated to be generated on PEP with the optic shown in Fig. 10 can in principle be generated without any special focussing by the LCLS. Although all of the above named research areas, together with an interferometry/imaging program aimed at exploiting the coherence properties of SR [13], are consequently still of extreme scientific interest, it is equally appropriate at this point to consider some of the implications of

extrapolating our developed microfocussing technology to the unfocussed LCLS beam.

As opposed to the cited exercise on Beam Line 5, which was limited by a relatively large source size, it is noteworthy to observe that the LCLS laser output will, by definition, be diffraction-limited. Consequently, a similar demagnification could be attempted to attain a diffraction-limited focus with a waist approaching the FEL wavelength. In order to assess the parameters associated with this feat, a log-log chart showing the equivalent energy density, power density, and field strength that could be attained at the focus is presented in Fig. 11. To emphasize the numbers involved, the Beam Line 5 experimental point is plotted along with equivalent numbers for an electron. With regard to the excitation of non-linear processes, we can recall that a standard criterion for assessing the strength of induced higher-order photon processes is the ratio of external field strength to the average field strength in an atom ($\approx 10^{10}$ V/m) [14]. Bearing in mind that high-power visible lasers can attain ratios of the order of 1, it is interesting to observe that the LCLS could, in principle attain ratios as high as 10^4. The implications are that a perturbation approach may no longer be applicable, and that new theoretical frameworks may have to be sought to predict experimental results. It seems noteworthy that we may well be within reach of investigating this speculation.

7. Acknowledgements

Useful discussions with members of the LCLS research group are acknowledged. This research was performed at SSRL which is operated by the Department of Energy, Office of Basic Energy Sciences, Division of Chemical Sciences. That Office's Division of Materials Sciences has provided support for this research.

8. References

[1] C. Pellegrini, J. Rosenzweig, H.-D. Nuhn, P. Pianetta, R. Tatchyn, H. Winick, K. Bane, P. Morton, T. Raubenheimer, J. Seeman, K. Halbach, K.-J. Kim, and J. Kirz, "A 2 to 4 nm High Power FEL on the SLAC Linac," presented at the 1992 FEL Conference, August 1992, Kobe, Japan; to appear in Nucl. Instr. and Meth. 1993.

[2] R. B. Palmer, "Prospects for High Energy e^+e^- Linear Colliders," Annu. Rev. Nucl. Part. Sci. 1990.40:529-92.

[3] B. L. Henke, P. Lee, T. J. Tanaka, R. L. Shimabukuro, and B. K. Fujikawa, "The Atomic Scattering Factor, $f_1 + if_2$, for 94 Elements and for the 100 to 2000 eV Photon Energy Region," AIP Conference Proceedings No. 75, 340(1982).

[4] G. A. Deis, A. R. Harvey, C. D. Parkinson, D. Prosnitz, J. Rego, E. T. Scharlemann, and K. Halbach, "A Long Electromagnetic Wiggler for the Paladin Free-Electron Laser Experiment," IEEE Trans. Mag. 24, 1090(1988).

[5] R. Tatchyn and H.-D. Nuhn, "A Comparison between the Coherence Parameters of Short Wavelength FELs Based on the SLAC Linac and Selected 2nd and 3d Generation Storage Ring Sources," elsewhere these proceedings.

[6] C. S. Fadley, "Research in Chemical Physics, Surface Science, and Materials Science, with a Linear Accelerator Coherent Light Source," elsewhere these proceedings.

[7] C. Shank, "The Prospect of Femtosecond X-Ray Pulses," elsewhere these proceedings.

[8] T. Raubenheimer and K. Bane, private communication.

[9] P. L. Csonka, "Suggested Method for Coherent X-Ray Production by Combined X-Ray and Low Energy Pumping," Phys. Rev. 13A(1), 405(1976).

[10] R. Tatchyn, P. Csonka, H. Kilic, H. Watanabe, A. Fuller, M. Beck, A. Toor, J. Underwood, and R. Catura, "Focusing of undulator light at SPEAR with a lacquer-coated mirror to power densities of 10^9 Watts/cm^2," SPIE Proceedings No. 733, 368(1987).

[11] R. Tatchyn, "The Potential of PEP as a High-Brightness Soft X-Ray Source for Coherence and Micro-Imaging Studies," Proceedings of the Workshop on X-Ray Microimaging for the Life Sciences, Berkeley, May 24-26, 1989, Report Nos. LBL-27660, UC-600, CONF-8905192, p. 185.

[12] R. Tatchyn, T. Cremer, and P. Csonka, "Design considerations for a new weak-field soft X-ray undulator/FEL driver for

PEP," Nucl. Instrum. Meth. A308, 152(1991).

[13] R. Tatchyn, E. Källne, A. Toor, T. Cremer, and P. Csonka, "Operation of a normal-incidence transmission grating monochromator at ALLADIN (invited)," Rev. Sci. Instrum. 60(7), 1579(1989).

[14] N. Bloembergen, Nonlinear Optics, W. A. Benjamin, Inc., London, 1965.

	DR Based		RF Gun Based								
	HYBRID UNDULATOR					PALADIN		FIELD SYNTHESIZER			
E	6.0 †	6.0 ‡	6.0	6.0	6.0	3.0	6.0	6.0	50.0	50.0	GeV
σ_t	12.4	12.4	5.0	5.0	6.0	9.8	5.0	5.0	4.0	4.0	$\times 10^{-4}$
ε_n	3.6	3.6	1.5	2.5	4.0	2.5	1.5	2.5	1.0	1.0	mm-mrad
$\varepsilon_{x,y}$	3.03	3.03	1.28	2.13	3.41	4.26	1.28	2.13	0.102	0.102	Å-rad
$\beta_{x,y}$	30.5	20.9	15	15	15	7.8	10	45	90	90	m
σ_s	1.8	1.8	0.2	0.2	0.2	0.2	0.2	0.2	0.1	0.1	ps
$\hat{I}$	0.7	0.7	2.4	2.4	2.4	2.4	2.4	2.4	5.0	5.0	kA
f_{rep}	12	12	120	120	120	120	120	120	120	120	Hz
$< I >$	0.038	0.038	0.14	0.14	0.14	0.14	0.14	0.14	0.3	0.3	μA
λ	140	40	40	40	40	40	10.6	40	1	1	Å
λ_u	10	5.1	10	10	10	8	8	36.1	36.1	20	cm
B_u	0.93	1.35	0.47	0.47	0.47	0.3	0.31	0.04	0.062	0.157	T
K_u	8.7	6.4	4.4	4.4	4.4	2.2	2.3	1.41	2.07	2.93	
z_R	8.3	20.2	6.1	10.2	16.4	15.1	10.3	29.5	115.36	115.36	m
ρ	11.4	7	19.5	16.5	14.1	18.8	13.2	19.9	8.45	7.18	$\times 10^{-4}$
ρ_{eff}	5.9	1.5	18.6	15.4	12.8	18.4	11.8	19.0	7.17	5.92	$\times 10^{-4}$
L_G	7.8	15.6	2.5	3.0	3.6	2.4	3.1	8.7	23.13	15.53	m
L_{sat}	170	339	54	65	78	44	68	190	503	337	m
σ_r	122	92.7	37	40.6	44.4	36.3	21.4	69.4	17.8	14.6	μm
$\sigma_{r'}$	9	3.44	8.6	7.8	7.67	8.8	3.95	4.58	0.446	.545	μrad
$\sigma_{Ix,Iy}$	155.3	122.2	57.4	69.6	84.2	68.1	41.7	120	35.1	33.6	μm
$\sigma_{Ix',Iy'}$	9.5	5.1	9.1	8.7	9.03	11.5	5.3	5.1	0.56	0.64	μrad
DIAM. @ 50m	3.6	3.1	1.9	1.96	2.2	2.24	1.22	2	0.51	0.43	mm §
DIAM. @ 250m	8.3	5.7	6.45	6.3	6.7	8	3.9	4.7	0.79	0.75	mm §
$\Delta\lambda_n/\lambda$	5.9	1.5	18.6	15.4	12.8	18.4	11.8	19.0	7.17	5.92	$\times 10^{-4}$
$\Delta\lambda_\perp/\lambda$	2	2	2	2	2	2	2	2	2	2	$\times 10^{-3}$ *
$(\Delta\lambda_n^2+\Delta\lambda_\perp^2)^{1/2}/\lambda$	2.09	2.006	2.73	2.52	2.37	2.72	2.322	2.76	2.13	2.09	$\times 10^{-3}$
P_{coh} ◊	2.5	0.63	26.7	22.1	18.5	11.7	17.0	27.3	179.3	148	GW
$<P_{coh}>$ ◊	0.135	0.34	1.6	1.33	1.11	0.7	1.02	1.64	5.38	4.45	W
N_{coh} ◊	8.0	0.57	2.7	2.2	1.9	1.16	0.45	2.75	0.23	0.186	$\times 10^{14}$/pls
$<N_{coh}>$ ◊	0.95	0.685	3.2	2.68	2.24	1.41	0.54	3.3	0.27	0.224	$\times 10^{16}$/s
$E_{\lambda(coh)}$ ◊	11.3	2.84	13.4	10.9	9.4	5.85	8.42	13.6	45.7	37.8	mJ
B	0.44	0.18	0.91	0.6	0.35	0.16	1.0	0.68	71	46.7	$\times 10^{21}$ ^
$< B >$	0.24	0.097	0.55	0.365	0.21	0.11	0.6	0.41	21.3	14.6	$\times 10^{21}$ ^

† Damping Ring (DR) energy 600 MeV; ‡ DR energy 600 MeV; § beam diameter at specified distance from end of undulator; ◊ over the entire inhomogeneous bandwidth; * 0.001 correlated energy spread in electron beam assumed; ^ [photons/sec,mm^2,mr^2,0.1%BW]

Figure 1. LCLS machine, electron beam, insertion device, photon output, and coherence parameters for various electron beam sources, spectral ranges, and insertion device types.

PARAMETERS FOR ASSESSING APPLICATIONS OF LINAC-BASED FEL RADIATION
(R. Tatchyn 3/26/92)

E [GeV]	(linac energy)
σ_ε	(relative energy spread)
ε_n	(normalized emittance)
$\varepsilon_{x,y}$ [nm-rad]	(vertical and horizontal emittances)
$\beta_{x,y}$ [m]	(vertical and horizontal beta functions)
σ_s [ps]	(standard deviation of temporal bunch length)
I [Amp]	(peak current in bunch)
f_{rep} [Hz]	(pulse repetition rate)
<I> [μA]	(average current)
λ [Å]	(first harmonic wavelength)
λ_u [cm]	(undulator period)
B_u [T]	(on-axis field amplitude)
K_u	(undulator deflection parameter)
z_R [m]	(Rayleigh length)
ρ	(ideal FEL gain parameter)
ρ_{eff}	(effective FEL gain parameter)
L_G [m]	(e-folding power gain length)
L_{sat} [m]	(undulator length for saturation)
σ_r [μm]	(diffraction-limited phot. beam size $(\lambda^{1/2}L_{sat}^{1/2}/4\pi)$)
$\sigma_{r'}$ [μrad]	(diffraction limited phot. beam angle $(\lambda/L_{sat})^{1/2}$))
$\sigma_{\Sigma x,\Sigma y}$ [μm]	(total phot. beam waist size)
$\sigma_{\Sigma x';\Sigma y'}$ [μrad]	(total phot. beam angle)
DIAM. @250m [mm]	(phot. beam diameter 250m from undulator center)
$\{\Delta\lambda/\lambda\}_h$	(homogeneously broadened bandwidth (= ρ_{eff}^{-1}))*
$\{\Delta\lambda/\lambda\}_i$	(inhomogeneously broadened bandwidth)*
P_{coh} [GW]	(peak coherent power over inh. BW)
$\langle P_{coh}\rangle$ [W]	(average coherent power over inh. BW)
N_{coh} [ph/pulse]	(peak coherent photons per pulse, over inh. BW)
$\langle N_{coh}\rangle$ [ph/s]	(average coherent photons per second, over inh. BW)
$E_{\lambda coh}$ [J]	(peak coherent energy in 1 pulse, over inh. BW)
B [ph/sec,mm^2,mr^2,0.1%BW]	(peak brightness)
<B> [ph/sec,mm^2,mr^2,0.1%BW]	(average brightness)

* if both profiles are assumed Gaussian, total BW = $(\Delta\lambda_h^2+\Delta\lambda_i^2)^{1/2}$).

Figure 2. Glossary for Figure 1.

SPECULAR REFLECTORS

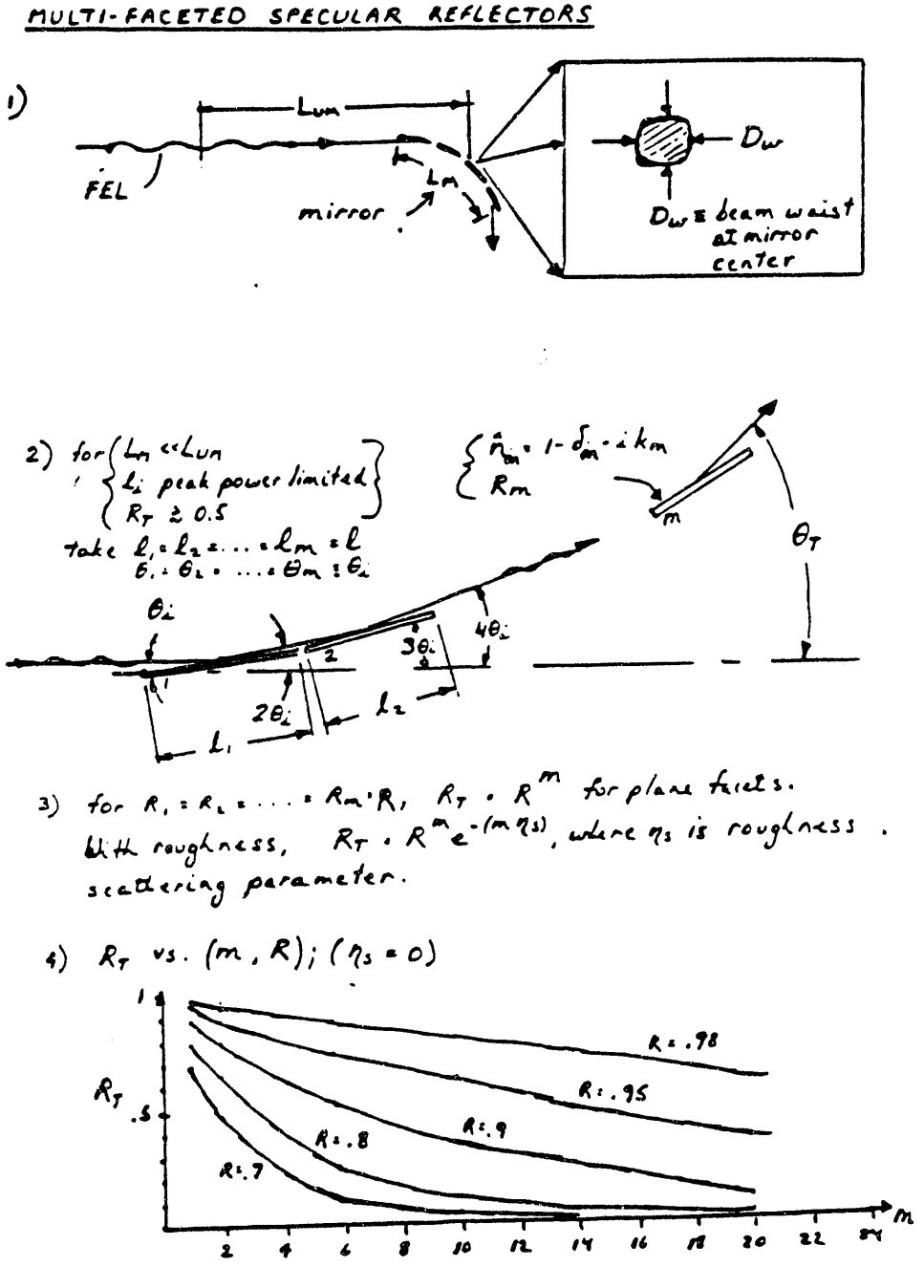

Figure 3. Beam and mirror facet parameters for multi-faceted reflectors.

DAMAGE ISSUES IN SPECULAR REFLECTORS

5) Define:

- δ_p ($\cong \frac{\lambda}{4\pi\sqrt{k}}$)
  ≡ 1/e penetration depth
- $\#\ [cm^{-3}]$ ≡ atomic density
- $\hat{P}_{col}\ [W]$ ≡ peak FEL power
- $\sigma_\tau\ [s]$ ≡ st. dev. of photon pulse length

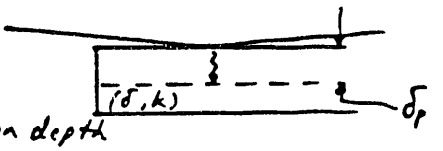

6) Introduce η_A, energy loading/atom
(when η_A is of the order of 1, it is known that surfaces can ablate)
Thus, introduce criterion for each mirror facet:

$$\eta_A \cdot \left(\frac{\hat{P}_{col}\sqrt{2\pi}\sigma_\tau}{g}\right)\left(\frac{\theta_i}{D_\omega^2}\right)\left(\frac{1-R}{\delta_p \#}\right) \ll 1 \qquad (1)$$

7) Example:
$\hat{P}_{col} = 10^{10}/2$; $\sigma_\tau = .2\times10^{-12}$; $D_\omega = 0.2$; $\# \cong 2\times10^{23}$;
$\delta_p \cong \lambda\ (= 40\text{Å})$; set criterion at $\eta_A \leq .01$

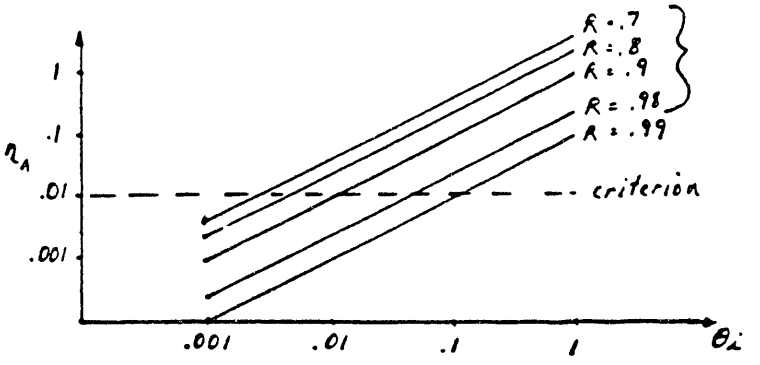

8) - BLS experiment attained ~ $10^9 w/cm^2$
(no definite ablation damage on Ni foils was observed)*

* R. Tatchyn et al, SPIE Proc. 733, p. 368 (1987)

Figure 4. Energy loading parameters and damage threshhold criteria for specular reflectors.

REFLECTIVITY AND SCATTERING

9) DESIGN:

- select θ_T, m for a given D_w
- $\ell = D_w/\theta_i$
- $\theta_i = \frac{1}{2}\theta_T/m$
- for θ_i small, mirror contour approximates a circle:

$$R_M = \frac{2m^2 D_w}{(\theta_T)^2} \quad (2)$$

$$\theta_M = \theta_T \quad (3)$$

$$L_m = m\ell \quad (4)$$

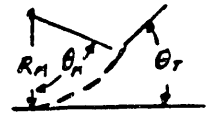

10) STUDY ($D_w = .2$ cm, use Al_2O_3 + Au constants *)

θ_T \ m		2	4	8	16
0.2 (~10°)	θ_i →	.05	.025	.0125	.00625
	L_m (m) →	.08	.32	1.28	5.12
	$R_T(Al_2O_3)$ →	0.9	0.85	0.82	0.8
	R_T(Au) →	0.29	0.31	0.31	0.25
0.4 (~22°)	θ_i →	.1	.05	.025	.0125
	L_m (m) →	.04	.16	.64	2.56
	$R_T(Al_2O_3)$ →	0.67	0.78	0.69	0.72
	R_T(Au) →	0.0225	0.079	0.08	0.015
0.8 (~45°)	θ_i →	.2	.1	.05	.025
	L_m (m) →	.02	0.08	.32	1.28
	$R_T(Al_2O_3)$ →	~0	0.45	0.61	0.44
	R_T(Au) →	~0	0.004	0.007	0.0015
1.6 (~90°)	θ_i →	.4	.2	.1	.05
	L_m (m) →	.01	.04	.16	.64
	$R_T(Al_2O_3)$ →	~0	~0	0.22	0.44
	R_T(Au) →	~0	~0	~0	~0

11) RESULTS WILL BE SENSITIVE TO SCATTERING PARAMETER η_s. FOR APPRECIABLE η_s, m must BE KEPT MINIMAL.

* from Hanle's compilation

Figure 5. Design study for a multifaceted reflector with facets of equal length, composed of either Au or Al_2O_3.

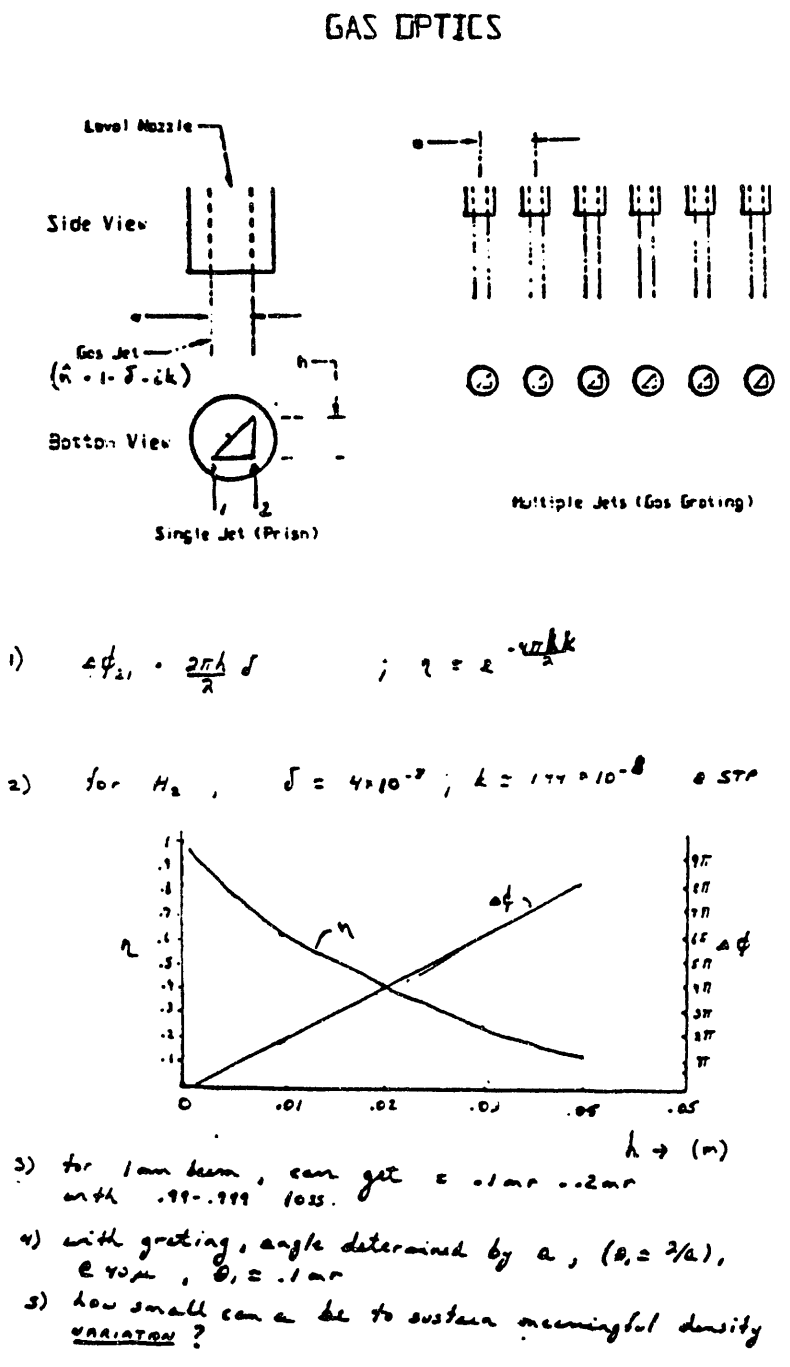

Figure 6. Gas-jet optical elements: gas prism (top left) and gas grating (top right). Attenuation and phase-gradient curves for an H_2 gas prism (bottom).

MONOCHROMATIZATION (Short-pulse limitations)

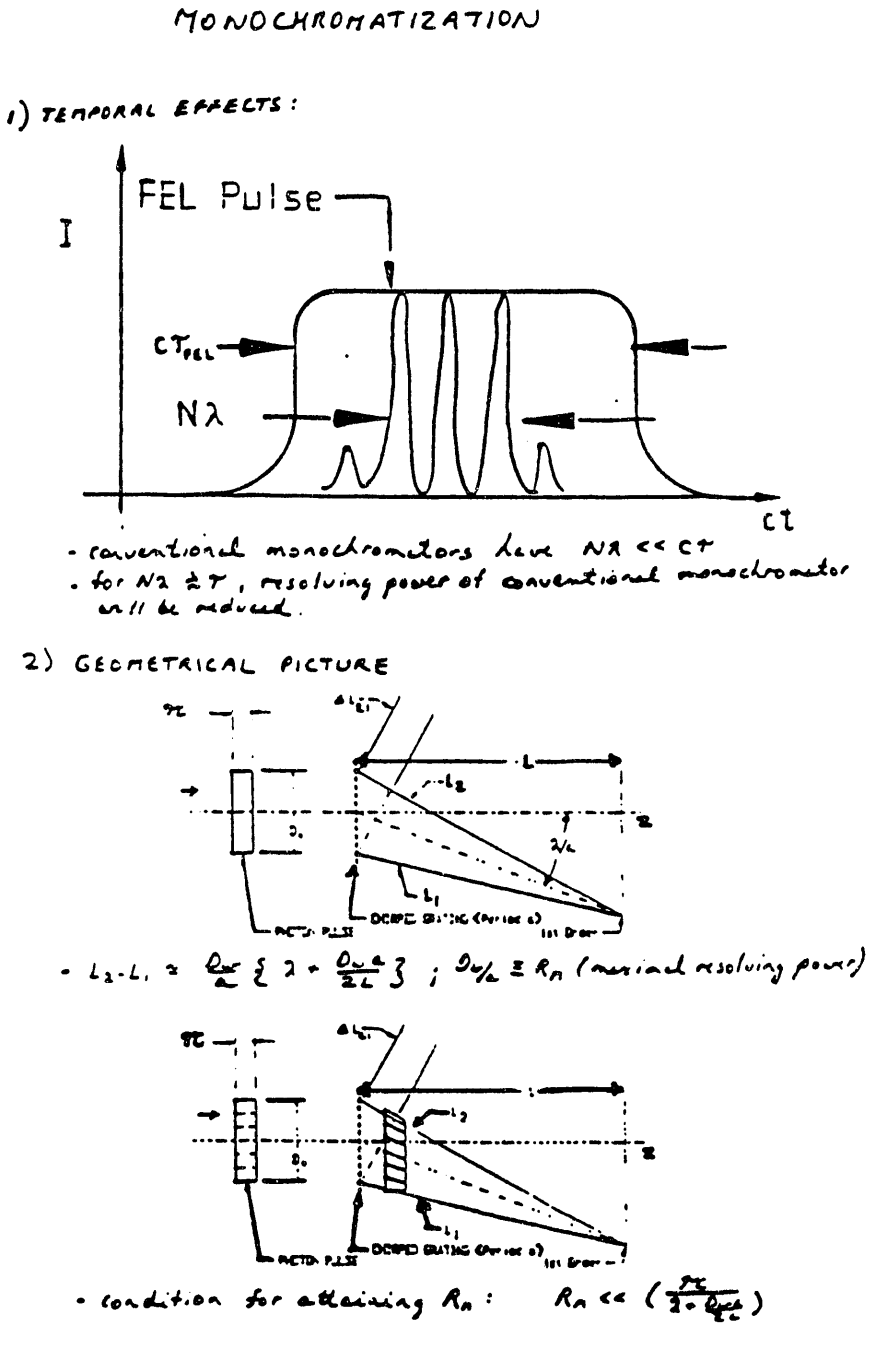

Figure 7. Aspects of Fourier-Transform-limited monochromatization. Temporal-spectral picture (top). Angular-spatial picture (bottom).

3) FOR GENERAL MONOCHROMATOR CONFIGURATION:

$$R \cong \left[\frac{1}{\left(\frac{1}{R_M}\right)^2 + \left(\frac{\lambda'}{Fc}\right)^2} \right]^{\frac{1}{2}} ; \quad \lambda' = \lambda + \frac{D_w a}{2L}$$

TABLE 1

R vs. τ[s] for $\lambda = 40$ Å ; $D_w = .002$m ; $\lambda/a = .01$; $L = 2$m

R_M \ τ		1.5×10^{-12}	0.3×10^{-12}	0.2×10^{-12}	0.1×10^{-12}
10^4	R =	9700	9100	8300	6000
5×10^3	R =	4960	4880	4700	4200
2.5×10^3	R =	~2500	~2500	2470	2371

4) CAN PHOTON PULSE BE LENGTHENED? SHORTENED?

METHODS: a) length dilation (contraction) of e⁻ beam in linac. Most effective.

b) dilation (contraction) of "correlated" energy gradient of e⁻ beam in linac. Implies loss.

Figure 8. Pulse-length loading of optimum monochromator resolving power. Formula (top). Case study (Table 1).

COMPRESSION

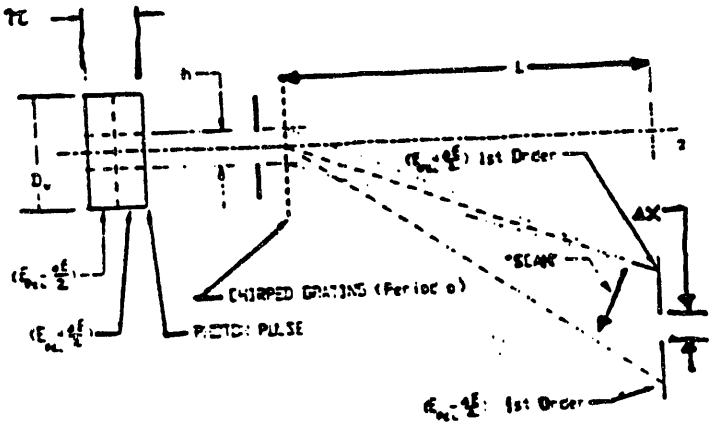

conditions: $\frac{1}{N_{(\lambda)}} \ll \frac{\Delta E_{FEL}}{\Delta E_{\lambda_w}} \simeq \frac{\Delta x\, c}{L(2\lambda_w - 2w)}$

TABLE 2.

$D_w = 0.001$ m ; $L = 2$ m ; $\frac{\Delta E_{FEL}}{E_{FEL}} \simeq 0.001$

λ_c[Å]	h[m]	N(h)	line density	$\frac{\Delta E_{1\lambda}}{\Delta E_{FEL}}$	$\frac{\Delta E_{loss}}{E_{LINAC}}$	λ_c[Å] loss fact.	
0.5	$\frac{0.001}{4}$	10	40 ℓ/mm	2	0.001	0.25	0.125
0.5	$\frac{0.001}{10}$	25	250 ℓ/mm	5	0.0025	0.1	2×10^{-2}
0.5	$\frac{0.001}{20}$	50	1000 ℓ/mm	10	0.005	0.05	5×10^{-3}
0.5	$\frac{0.001}{40}$	100	4000 ℓ/mm	20	0.01	0.025	1.25×10^{-3}
0.5	$\frac{0.001}{80}$	200	16,000 ℓ/mm	40	0.02	0.0125	3.1×10^{-4}

Figure 9. Pulse compression based on chirped photon bunch energy. The front of the bunch diffracts into a smaller angle than the rear. A small slit Δx placed between the two extremes will filter out a temporally abbreviated slice of the original pulse as it scans between the extremes.

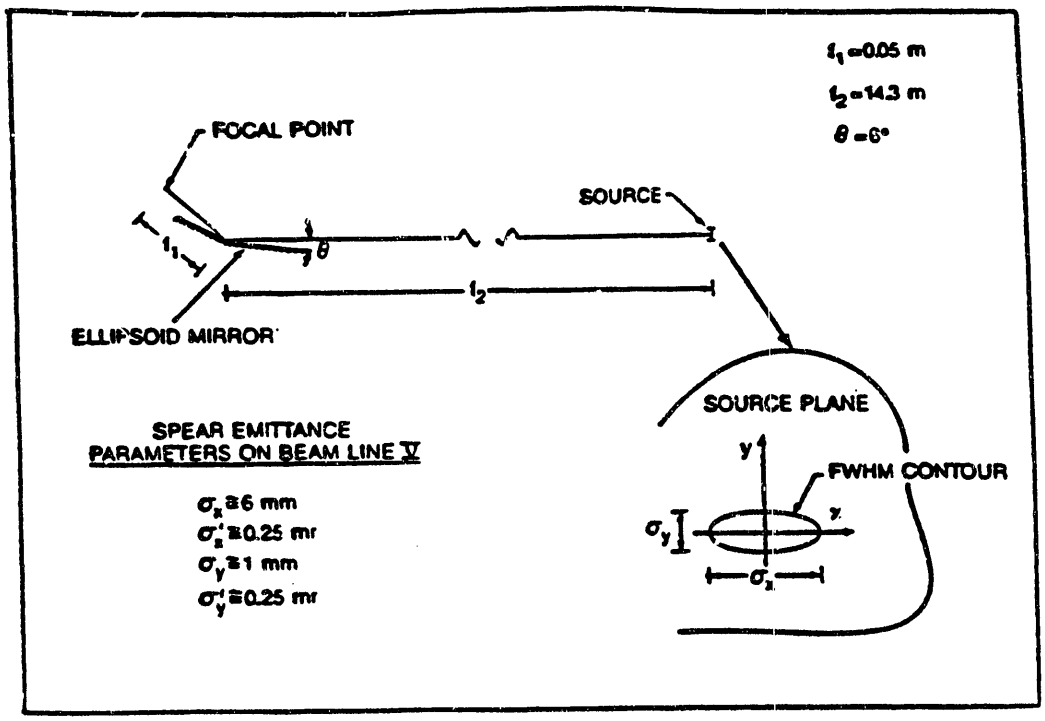

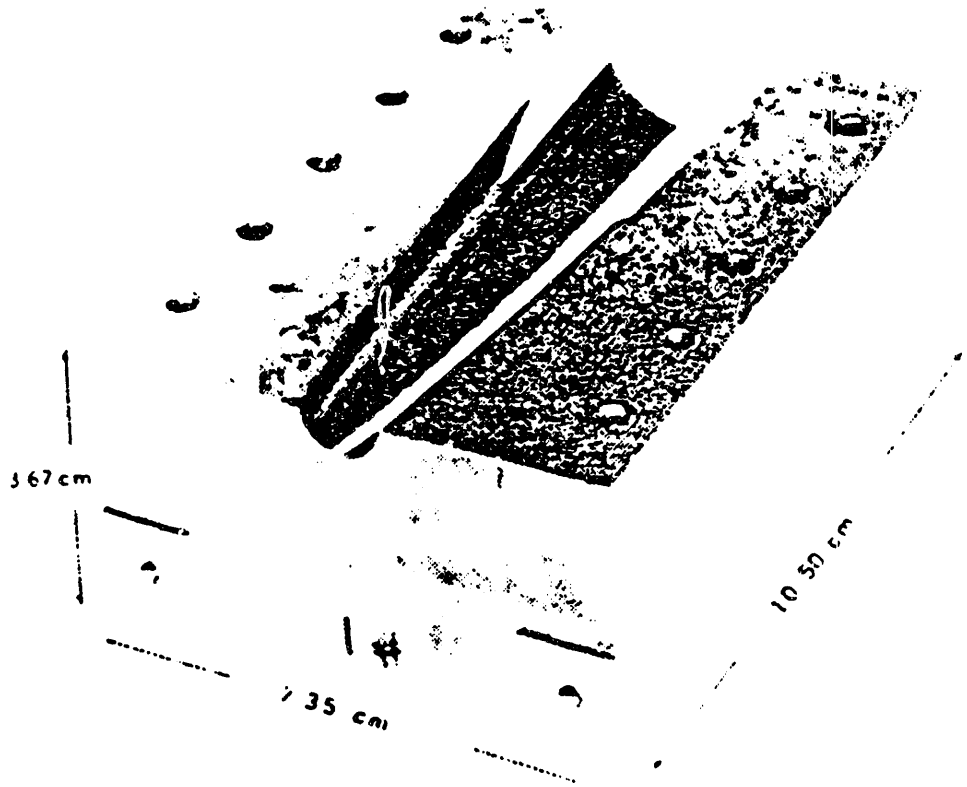

Figure 10. Microfocussing geometry on Beam Line 5 on SPEAR with a specular ellipsoidal reflector (top). Diamond-turned, lacquer-coated, and metallized ellipsoid (bottom). Defocussing ratio 300:1.

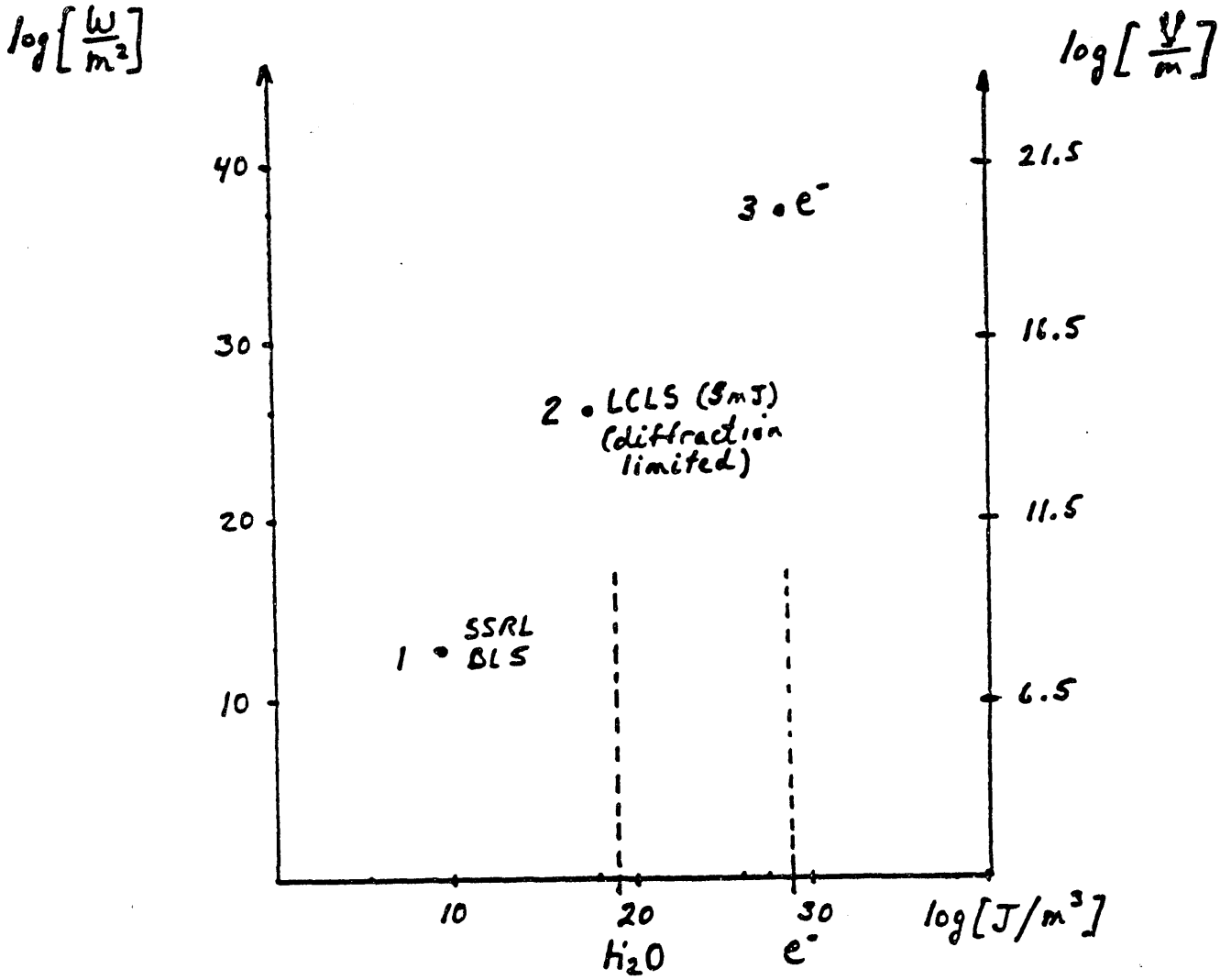

Figure 11. Equivalent field strengths and energy densities attained: 1) with ellipsoidal reflector on Beam Line 5 on SPEAR; 2) at the diffraction-limited focus of the LCLS FEL; and 3) at the classical radius of an electron. The equivalent energy densities of water and electronic matter are marked on the abscissa.

END

DATE
FILMED
6/17/93